**Rare Metal Materials and Engineering**
Volume 53, Issue 3, March 2024
Available online at www.rmme.ac.cn

Science Press

**Cite this article as**: Zhao Ligong, Li Jianghao, Guo Huijuan, et al. Effect of Palladium Electroplating on Hydrogen Absorption Properties of Zirconium Alloy[J]. Rare Metal Materials and Engineering, 2024, 53(03): 685-691. DOI: 10.12442/j.issn.1002-185X.20230102.

ARTICLE

# Effect of Palladium Electroplating on Hydrogen Absorption Properties of Zirconium Alloy

**Zhao Ligong[1], Li Jianghao[1], Guo Huijuan[2], Yang Dawen[3], Zhang Anjia[3], Zhang Peilong[3], Zhou Wenjiao[1], Tong Huan[1], Song Xiping[1]**

*[1] State Key Laboratory for Advanced Metals and Materials, University of Science and Technology Beijing, Beijing 100083, China; [2] CNPC Engineering Technology R&D Company Limited, Beijing 102206, China; [3] Whole Win (Beijing) Materials Sci. and Tech. Co., Ltd, Beijing 102100, China*

**Abstract:** Zirconium is an excellent hydrogen absorption material and has been regarded as a candidate material in the deuterium storage field. However, due to its higher hydrogen absorption temperature and slower hydrogen absorption kinetics, it cannot be applied at present. Palladium electroplating was used as a surface modification to improve the property. The results show that after the palladium electroplating and annealing, the zirconium alloy can absorb hydrogen at room temperature with an appropriate incubation period. With the increase in temperature, the hydrogen absorption rate becomes faster with a shorter incubation period. A transition zone forms between the palladium layer and zirconium substrate, and $PdH_{1.33}$ and $H_{0.62}Zr_{0.38}$ are found in the transition zone after hydrogenation. These hydride phases in the transition zone play an important role in improving the hydrogen absorption property of zirconium. For the kinetics mechanism, it is determined to be 1-D diffusion at room temperature and 2-D diffusion at 250 °C.

**Key words:** zirconium; palladium electroplating; hydrogen absorption temperatures; hydrogen absorption kinetics

Energy is one of the most significant problems which directly affects the survival and development of human beings. With the shortage of fossil fuels and the serious environmental pollution, nuclear energy has attracted much attention[1]. The current nuclear energy is mainly focused on nuclear fission energy, while safety and nuclear waste of nuclear fission reaction remain a thorny issue and difficult to solve[2]. In contrast, another form of nuclear energy, nuclear fusion energy has attracted much attention due to its controllability and cleanness[3–5]. In addition, its energy is 2−3 times higher than that of nuclear fission energy. Thus, the development of nuclear fusion energy is very necessary and urgent.

It is known that the fusion reaction is ${}_1^2H + {}_1^3H \rightarrow {}_2^4He + {}_0^1n$. Deuterium (${}_1^2H$) is one part of the main fusion reactor fuels, and its preparation, storage and recycling are very important issues restraining its practical application[6–7]. Commonly, deuterium is produced from heavy water, which is abundant in the ocean water, and is stored in uranium material[8–10]. The uranium has a high storage capacity, good stability at room temperature, and quick release rate at high temperature[11], while there are some problems with uranium, which possesses serious pulverization and pyrophoricity after several deuterium absorption/desorption cycles[12]. Therefore, it is necessary to find out another material to replace uranium.

Zirconium is an excellent hydrogen absorption material and has been regarded as a candidate material in the deuterium storage field, due to its greater hydrogen storage capacity and excellent stability at room temperature[13–21]. However, because of its higher hydrogen absorption temperature, which is above 450 °C, and slower hydrogen absorption kinetics[22], its application has been restricted to some extent.

In order to reduce the hydrogen absorption temperature of zirconium, palladium modification is an effective way[23–26]. Since palladium has a strong catalytic effect on the

Received date: March 01, 2023
Foundation item: National Natural Science Foundation of China (21171018, 51271021); Supported by State Key Laboratory for Advanced Metals and Materials (2019-ZD06, 2021Z-18)
Corresponding author: Song Xiping, Ph. D., Professor, State Key Laboratory for Advanced Metals and Materials, University of Science and Technology Beijing, Beijing 100083, P. R. China, Tel: 0086-10-62333213, E-mail: xpsong@skl.ustb.edu.cn

dissociation/adsorption of hydrogen[27–32], it is used as surface catalytic to improve the hydrogen absorption property of zirconium alloy. In this study, a significant electroplating process, which is more efficient and convenient, was employed to improve the hydrogen absorption property of zirconium. The microstructure, phase structure, and the hydrogen absorption properties were investigated, and the apparent activation energy and the diffusion mechanism of palladium electroplating zirconium alloy were also investigated.

## 1 Experiment

Zr-4 material was provided by Western New Zirconium Nuclear Material Technology Co., Ltd. Square samples with 10 mm in length and 1 mm in thickness were machined by wire cutting from Zr-4 sheets. Both sides of the square samples were mechanically polished and rinsed with ethanol, and then electroplated as the negative electrode in an electroplating bath, with the graphite as the positive electrode. The plating solution consists of $1.0\times10^{-2}$ mol $PdCl_2$, 4.8 $g\cdot L^{-1}$ ethylenediamine and 11 $g\cdot L^{-1}$ $N_2H_4\cdot H_2O$. The electroplating time was 20 min, and the electroplating current was 0.05 A. After electroplating, the samples were annealed at 500, 600, and 700 °C in vacuum for 4 h. The purpose of annealing is to improve the densification of the palladium film and the bonding ability with zirconium[33].

Hydrogen absorption experiments were carried out in a Sievert's device. In order to determine the onset temperature of hydrogen absorption, the samples were firstly activated by heating from 25 °C to 500 °C at a step of 50 °C. At each heating temperature step, the samples were kept for 10 min under the hydrogen pressure of 0.05 MPa. After the cycle, the samples were heated to 600 °C to desorb hydrogen in vacuum. Then, the samples were recharged with hydrogen again for the second and the third cycles to determine the decrease in the onset temperature. After this activation process, the kinetics of hydrogen absorption of the samples was tested under the hydrogen pressure of 0.2 MPa beyond the onset temperature. For the kinetics testing, three temperatures (room temperature, 150 °C, as well as 250 °C) were chosen, and the samples were heated to these temperatures in vacuum and kept for 30 min, and then the hydrogen gas was charged for hydrogen absorption at the hydrogen pressure of 0.2 MPa. The hydrogen absorption time was planned to be 0.5 h for all samples. Finally, the samples were cooled down to room temperature by the furnace cooling in the hydrogen atmosphere. The hydrogen absorption amount was consequently calculated by the ideal gas equation.

The phase structures before and after the hydrogen absorption were analyzed by Rigaku TTRIII X-ray diffractometer (XRD), using Cu Kα with a step of 0.02° and counting time of 1 s/step. The microstructure was characterized by scanning electron microscope (SEM). The morphology of the samples after hydriding was investigated by FEI Tecnai F30 at an accelerating voltage of 300 kV. The TEM samples were prepared by FIB technology (Zeiss Auriga).

In order to obtain the hydrogen absorption mechanism, the hydrogen absorption fraction $\alpha$ was calculated by $\alpha = (P_0 - P_t)(P_0 - P_f)$, where $P_0$ is the initial hydrogen pressure in the chamber before absorption starts, $P_t$ is the pressure during absorption at the time $t$, and $P_f$ is the final pressure in the chamber. The kinetic data of $\alpha$ and $t$ were fitted into different mechanism functions, $g(\alpha) = kt$, with the $\alpha$ values ranging from 0.1 to 0.9. The mechanism function, which has the best linear fitting vs $t$, was considered to be the mechanism function of the hydrogen absorption kinetic. Different mechanism functions $g(\alpha)$ can be obtained from Ref.[34].

## 2 Results and Analysis

### 2.1 Microstructure characterization

Fig. 1 shows the surface morphologies of the palladium electroplating zirconium samples, together with the palladium electroplating zirconium samples annealed at 500, 600, and 700 ° C. It can be seen that after annealing, the surface palladium film becomes denser compared with that of the unannealed samples. In Fig. 1a, it can be seen that surface palladium film has a porous microstructure, but with the increase in the annealing temperature, (Fig. 1b – 1d), the palladium film becomes more compact, with smaller micropores on the surface.

The XRD patterns of zirconium sample, palladium electroplating zirconium sample as well as annealed palladium electroplating zirconium samples are shown in Fig.2. It can be seen from Fig. 2a that after electroplating, except the diffraction peaks of zirconium, diffraction peaks of palladium also appear at 40° and 46° for the palladium electroplating zirconium samples. After annealing at different temperatures, as shown in Fig.2b, it can be seen that with the increase in the annealing temperature, the phase component of palladium electroplating zirconium sample is changed. After annealing at 500 °C, only Zr and Pd phases are detected, which is the same as that of the unannealing samples. After annealing at 600 °C, a new phase of $PdZr_2$ is found. After annealing at 700 °C, another new phase of $Pd_3Zr_6O$ phase appears, and the diffraction peaks of palladium and $PdZr_2$ phase disappear. Thus, in order to maximize the role of palladium, annealing at 500 °C is selected as the optimal annealing process for the preparation of follow-up hydrogen absorption samples.

### 2.2 Hydrogen absorption property

Fig. 3 shows the activation curves of zirconium and palladium electroplating zirconium samples for different cycles. As can be seen from Fig. 3a, with the increase in cycles, the hydrogen absorption temperature of zirconium samples keeps almost the same at about 450 °C. However, in Fig. 3b, with the increase in cycles, the hydrogen absorption temperatures of palladium electroplating Zr samples decrease significantly. The hydrogen absorption temperature is 450 °C at the first cycle, while it decreases to 150 °C at the second cycle, and further decreases to the room temperature at the third cycle. This result indicates that the palladium

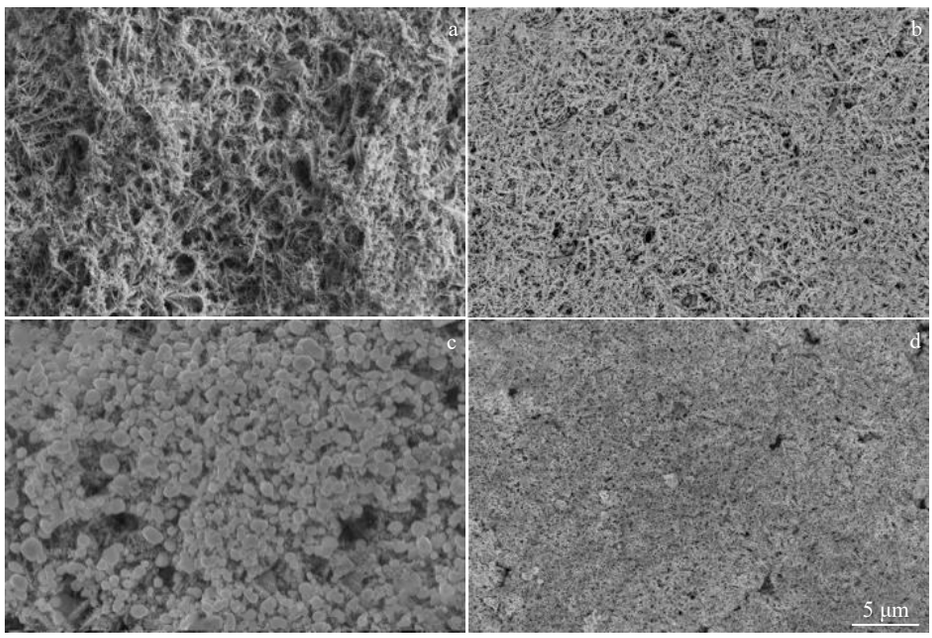


Fig.1 Surface morphologies of the palladium electroplating zirconium samples before (a) and after annealing at 500 °C (b), 600 °C (c), and 700 °C (d)

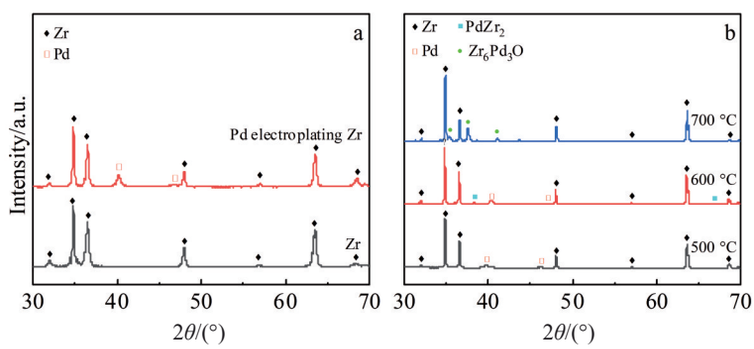


Fig.2 XRD patterns of zirconium sample and palladium electroplating zirconium sample (a) and palladium electroplating zirconium samples annealed at different temperatures (b)

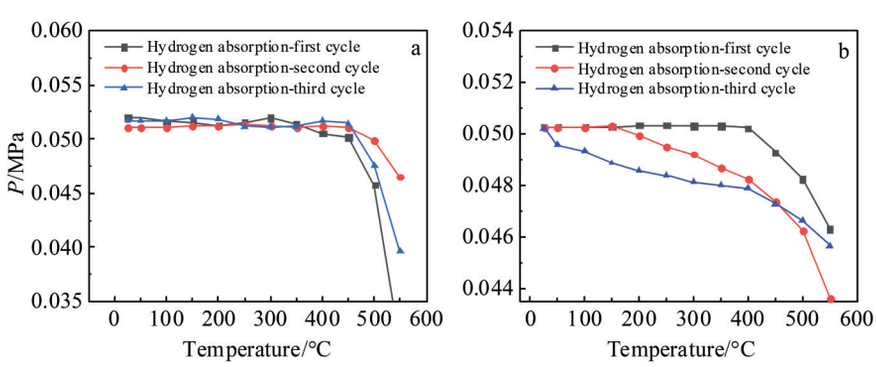


Fig.3 Activation curves of zirconium (a) and palladium electroplating zirconium (b) for different cycles

electroplating has a significant catalytic effect on the onset temperature of hydrogen absorption, and makes it decrease with the hydrogen absorption cycles.

### 2.3 Hydrogen absorption kinetics

It can be concluded from the above results that the zirconium after palladium electroplating can absorb hydrogen at room temperature. In order to further understand its hydrogen absorption property, the hydrogen absorption kinetics of palladium electroplating zirconium annealed at 500 °C were evaluated.

Fig. 4a – 4c show the hydrogen absorption kinetics of zirconium and palladium electroplating zirconium at 25, 150 and 250 °C under the hydrogen pressure of 0.2 MPa after the activation. It can be seen that palladium electroplating zirconium samples have a better hydrogen absorption kinetics than zirconium samples at all temperatures. By the comparison of palladium electroplating zirconium samples at different temperatures (Fig. 4d), it can be seen that with the increase in hydrogen absorption temperature, hydrogen absorption kinetics become fast, almost without incubation period at 250 °C.

The kinetics mechanisms of the hydrogen absorption for the palladium electroplating zirconium samples at different temperatures are evaluated by the fitting of the data using the kinetics mechanism functions. The results are shown in Fig.5a and Table 1. It can be seen from Fig. 5a that the hydrogen absorption mechanisms at 150 and 250 °C follow the 2-D diffusion mechanism, which is expressed as $g(\alpha)=\alpha+(1-\alpha)\times[\ln(1-\alpha)]=kt$, where $k$ is rate constant, and $t$ is time. The hydrogen absorption mechanism at room temperature follows the 1-D diffusion mechanism, which is expressed as $g(\alpha)=\alpha^2=kt$. It demonstrates that the kinetics, mechanisms of hydrogen absorption in the palladium electroplating zirconium at different temperatures are all diffusion mechanism, but it is transformed from 2-D to 1-D diffusion with the decrease in temperature. The value of rate constant $k$ in the diffusion equation also increases with the increase in temperature, as seen in Table 1, which can be used to calculate the apparent activation energy ($E_a$) of the hydrogen absorption. Based on the Arrhenius equation, $k=A\exp(-E_a/RT)$ , i. e., by plotting

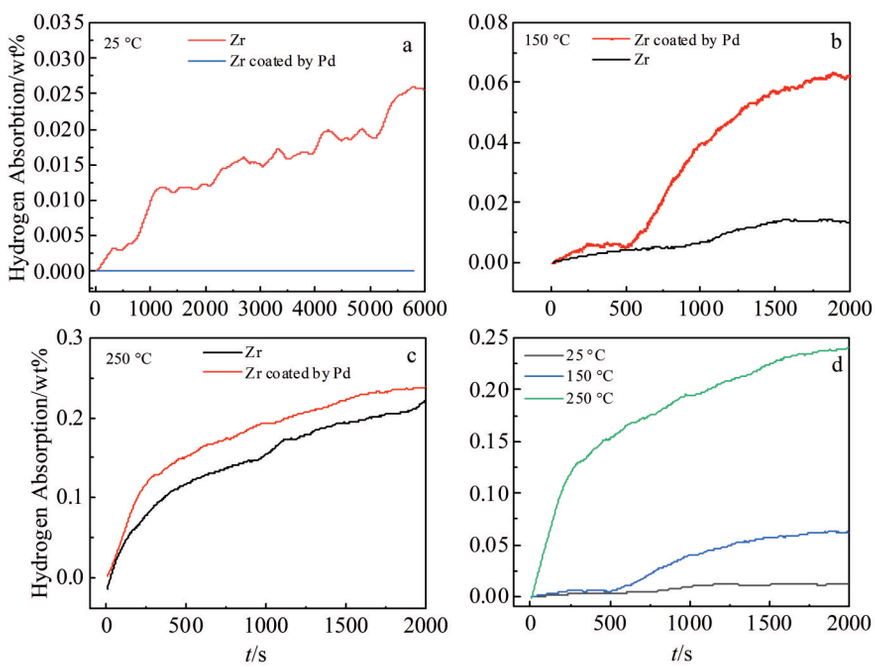


Fig.4 Hydrogen absorption kinetics of zirconium and annealed palladium electroplating zirconium at 25 °C (a), 150 °C (b), and 250 °C (c) after activation; comparison of hydrogen absorption kinetics of palladium electroplating zirconium at different temperatures (d)

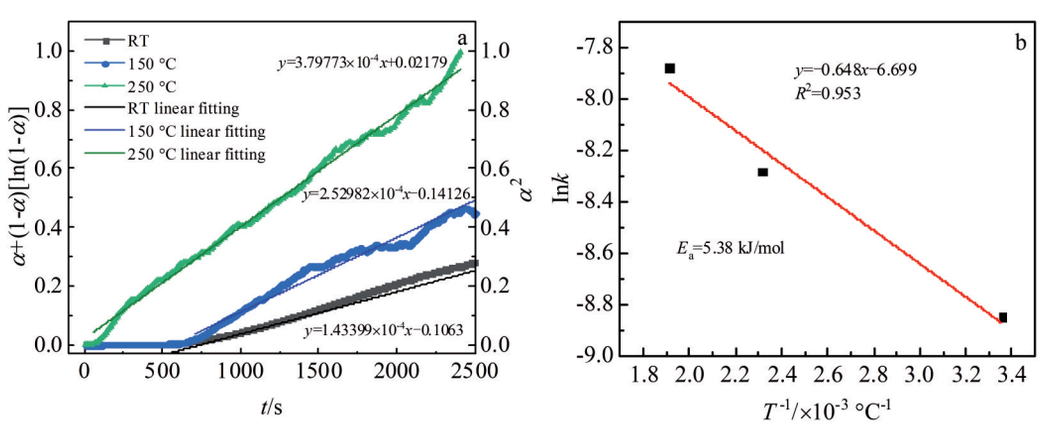


Fig.5 Hydrogen absorption kinetics mechanism function fitting of palladium electroplating zirconium at different temperatures (a) and plots of $\ln k$ vs $1/T$ (b)

**Table 1 Kinetics fitting results of palladium electroplating zirconium samples hydrogenated at different temperatures**

| Condition | Diffusion model | $g(\alpha)$ | $k/\times10^{-4}$ s$^{-1}$ |
|---|---|---|---|
| 25 °C, 0.2 MPa | 1-D | $\alpha^2=kt$ | 1.434 |
| 150 °C, 0.3 MPa | 2-D | $\alpha+(1-\alpha)[\ln(1-\alpha)]=kt$ | 2.530 |
| 250 °C, 0.4 MPa | 2-D | $\alpha+(1-\alpha)[\ln(1-\alpha)]=kt$ | 3.780 |

ln$k$ versus 1/$T$ curves, as shown in Fig. 5b, the $E_a$ of the palladium electroplating zirconium samples is determined to be 5.38 kJ/mol.

The phase component of the palladium electroplating zirconium sample after hydrogen absorption at 250 ° C is shown in Fig.6. It can be seen that both the surface palladium and the matrix zirconium are hydrogenated to form their corresponding hydrides, which are $PdH_{1.33}$ and $ZrH_2$, together with $H_{0.62}Zr_{0.38}$ phase formed.

TEM morphologies of the samples after hydriding at 250 °C are shown are Fig.7. Fig.7a shows the HAADF-STEM image of the cross section of sample from the palladium film to zirconium substrate. Three layers can be observed: surface palladium film, transition zone and zirconium substrate. The thickness of transition zone is around 1 μm. Fig.7b shows the diffraction ring of Pd layer, which proves that the surface palladium film exists and no palladium hydrides appear. Fig. 7c shows corresponding HRTEM image. Obviously, the transition zone contains two kinds of hydride phases: $PdH_{1.33}$ and $H_{0.62}Zr_{0.38}$. Fig. 7d shows the diffraction pattern of the zirconium substrate, which indicates that the zirconium substrate has been completely hydrogenated to the $ZrH_2$ phase. According to TEM results, it is confirmed that a transition zone is indeed formed after hydrogen absorption in samples annealed at 500 °C.

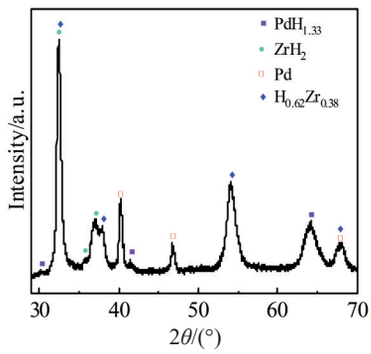


Fig.6 XRD pattern of palladium electroplating zirconium sample after hydrogen absorption at 250 °C

## 3 Discussion

In this study, it has been found that the palladium electroplating zirconium sample exhibits an excellent hydrogen absorption property, which can absorb hydrogen at room temperature, as shown in Fig. 4a. The reason for this is related with the palladium film and the palladium-zirconium transition zone. As we know, palladium is characterized by its ability to absorb the hydrogen at room temperature[35], so with surface palladium film, the hydrogen molecules can be easily dissociated into hydrogen atoms and transferred to the palladium-zirconium interface. At the palladium-zirconium interface, due to the annealing treatment, a palladium-zirconium transition zone forms. Inside this transition zone,

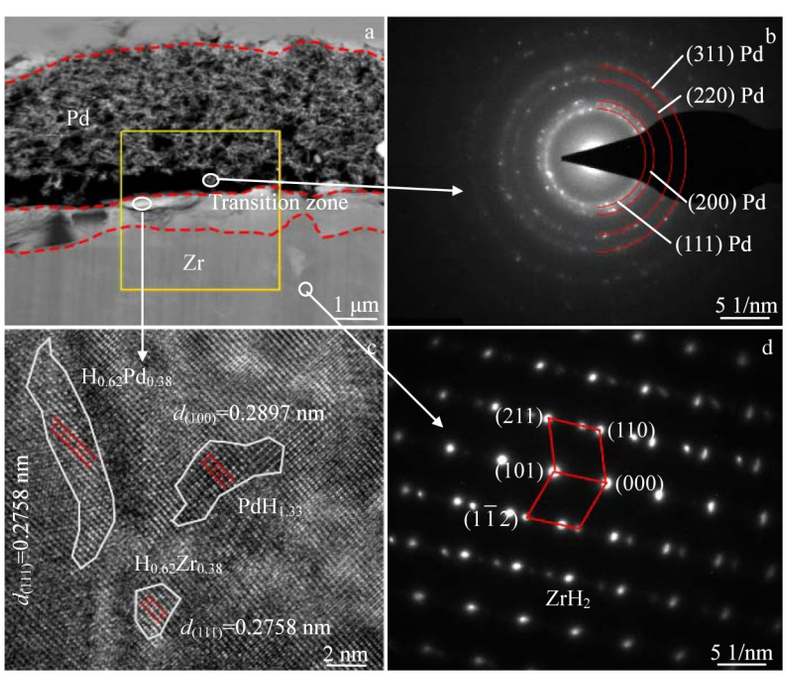


Fig.7 TEM images of palladium electroplating zirconium samples after hydrogen absorption at 250 ° C: (a) HAADF-STEM image, (b) diffraction ring of Pd layer, (c) HRTEM image of the transition layer, and (d) diffraction pattern of the zirconium matrix

the nano palladium hydrides form after activation and act as a channel into Zr substrate, which makes the hydrogen atom diffuse from palladium phase to zirconium phase directly, and thus the zirconium can absorb the hydrogen at room temperature. This is a new discovery for the opinion that the zirconium can absorb the hydrogen above 450 °C.

At room temperature, due to the discontinuous $PdH_{1.33}$ phase in the transition zone, the hydrogen atoms diffuse along a one-dimensional channel, which coincides with the result of one-dimensional diffusion mechanism. The schematic diagram of one-dimensional diffusion mechanism is shown in Fig. 8a. At 250 ° C, a large number of $PdH_{1.33}$ phases form which allow the hydrogen diffusion along multiple channels in a "fluid-like" manner[36], becoming a two-dimensional diffusion mechanism. And the schematic diagram of two-dimensional diffusion mechanism is shown in Fig.8b.

A comparison of the apparent activation energy ($E_a$) between the palladium electroplating Zr and some traditional hydrogen storage alloys, such as $AB_5$[37], AB[38], $AB_2$[39] and pure Zr alloys in hydrogen absorption is presented in Table 2. It can be seen that the palladium electroplating Zr in this study has the lowest apparent activation energy of 5.38 kJ/mol compared with the traditional hydrogen storage alloys. Therefore, the surface palladium film can significantly reduce the apparent activation energy of zirconium, resulting in hydrogen absorption at room temperature. This excellent property of the palladium electroplating Zr which absorbs hydrogen at room temperature opens up a new application field of zirconium, making it more available to use as a deuterium storage material as well as a deuterium-recovered material at room temperature.

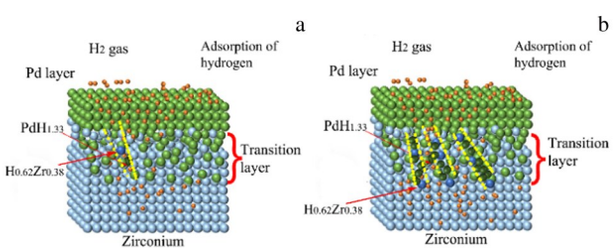


Fig.8 Schematic diagrams of diffusion mechanism: (a) one-dimensional at room temperature and (b) two-dimensional diffusion at 250 °C

**Table 2 Comparison of apparent activation energy ($E_a$) between palladium electroplating Zr and traditional hydrogen storage alloys in hydrogen absorption**

| Alloy | $E_a$/kJ·mol$^{-1}$ | Condition |
|---|---|---|
| $LaNi_5$ | 13.2 | 0.5 MPa, 293 K |
| TiFe | 7.53 | 2.5 MPa, 294 K |
| $Ti_{0.1}Zr_{0.9}Mn_{0.9}V_{0.1}Fe_{0.5}Ni_{0.5}$ | 21.2 | 2 MPa, 323 K |
| Pure Zr | 41.51 | 0.24 MPa, 773K |
| Palladium electroplating Zr | 5.38 | 0.2 MPa, 293 K |

## 4 Conclusions

1) After palladium electroplating and annealing, the onset hydrogen absorption temperature of the zirconium alloy drops to room temperature, and the hydrogen absorption kinetics is significantly improved.

2) The reason for hydrogen absorption of palladium electroplating zirconium alloys at room temperature is the formation of intermediate phases $PdH_{1.33}$ and $H_{0.62}Zr_{0.38}$ at the transition zone between palladium film and zirconium substrate.

3) The hydrogen absorption mechanism at room temperature is determined to be 1-D diffusion mechanism, while it is determined to be 2-D diffusion mechanism at 250 °C.

## References

1 Nowotny J, Hoshino T, Dodson J *et al. Hydrogen Energy*[J], 2016, 41(30): 12812
2 Zhiznin S Z, Timokhov V M, Gusev A L. *Hydrogen Energy*[J], 2020, 45(56): 31353
3 Shuai M, Su Y, Wang Z *et al. Nucl Mater*[J], 2002, 301(2–3): 203
4 Dou N, Song X, Yang Y *et al. Rare Metal Materials and Engineering*[J], 2016, 45(1): 97
5 Dou N, Song X, Yang Y *et al. Rare Metal Materials And Engineering*[J], 2016, 45(3): 667
6 Graham T. *Franklin Inst*[J], 1867, 83(1): 39
7 Chang M H, Yun S H, Kang H G *et al. Fusion Eng Des*[J], 2014, 89(7–8): 1557
8 Kanouff M P, Gharagozloo P E, Salloum M *et al. Chem Eng Sci*[J], 2013, 91: 212
9 Shugard A D, Buffleben G M, Johnson T A *et al. Nucl Mater*[J], 2014, 447(1–3): 304
10 Asada K, Ono K, Yamaguchi K *et al. Alloys Compd*[J], 1995, 231(1–2): 780
11 Yang Y, Song X, Zhang C. *Hydrogen Energy*[J], 2016, 41(47): 22206
12 Ablitzer C, Le G F, Raynal J *et al. Nucl Mater*[J], 2013, 432(1–3): 135
13 Conić D, Gradišek A, Radaković J *et al. Hydrogen Energy*[J], 2015, 40(16): 5677
14 Zhao C, Song X, Yang Y *et al. Hydrogen Energy*[J], 2013, 38(25): 10903
15 Juillet C, Tupin M, Martin F *et al. Hydrogen Energy*[J], 2021, 46(11): 8113
16 Zhang C, Song A, Yuan Y *et al. Hydrogen Energy*[J], 2020, 45(8): 5367
17 Zhang B, Wang F, Cheng J *et al. Hydrogen Energy*[J], 2021, 46(80): 40217
18 Begrambekov L B, Evsin A E, Grunin A V *et al. Hydrogen*

*Energy*[J], 2019, 44(31): 17154
19 Kashkarov E B, Nikitenkov N N, Sutygina A N *et al. Hydrogen Energy*[J], 2018, 43(4): 2484
20 Zhang Yin, Zhang Cheng, Yuan Gaihuan *et al*. *Rare Metal Materials and Engineering*[J], 2019, 48(8): 2602 (in Chinese)
21 Zhang Yin, Zhang Cheng, Yuan Gaihuan *et al*. *Rare Metal Materials and Engineering*[J], 2019, 48(8): 2507 (in Chinese)
22 Cekić B, Ćirić K, Iordoc M *et al. Alloys Compd*[J], 2013, 559: 162
23 Chen W H, Chen K H, Kuo J K *et al. Hydrogen Energy*[J], 2022, 47(100): 42266
24 Zhao B, Liu L, Ye Y *et al. Hydrogen Energy*[J], 2016, 41(5): 3465
25 Zhang T, Zhang Y, Zhang M *et al. Hydrogen Energy*[J], 2016, 41(33): 14778
26 Wang F, Liu J, Liang L *et al. Hydrogen Energy*[J], 2022, 47(17): 9946
27 Satawara A M, Gupta S K, Andriotis A N *et al. Hydrogen Energy*[J], 2022, 47(44): 19132
28 Jokar S M, Farokhnia A, Tavakolian M *et al. Hydrogen Energy*[J], 2023, 48(16): 6451
29 Heller E M B, Vredenberg A M, Boerma D O. *Appl Surf Sci*[J], 2006, 253(2): 771
30 Gautam Y K, Chawla A K, Walia R *et al. Appl Surf Sci*[J], 2011, 257(14): 6291
31 Chen W H, Chen Z Y, Lim S *et al. Hydrogen Energy*[J], 2021, 47(96): 40787
32 Adams B D, Chen A. *Mater Today*[J], 2011, 14(6): 282
33 Ozaki T, Zhang Y, Komaki M *et al*. *International Journal of Hydrogen Energy*[J], 2003, 28(3): 297
34 Khawam A, Flanagan D R. *Phys Chem B*[J], 2006, 110(35): 17315
35 Du X, Ye X, Chen C *et al. Hydrogen Energy*[J], 2021, 46(1): 1023
36 Kehr K W. *Electronic Structure and Properties of Hydrogen in Metais*[M]. Boston: Springer, 1983: 531
37 Kitada M. *Japan Inst Met*[J], 1977, 41(4): 412
38 Choong-Nyeon P, Jai-Young L. *Less Common Met*[J], 1983, 91(2): 189
39 Kandavel M, Ramaprabhu S. *Phys Condens Matter*[J], 2003, 15(44): 7501

# 电镀钯对锆合金吸氢性能的影响

赵立功[1]，李江豪[1]，郭慧娟[2]，杨大稳[3]，张岸佳[3]，张沛龙[3]，周文娇[1]，佟　欢[1]，宋西平[1]

(1. 北京科技大学 新金属材料国家重点实验室，北京 100083)

(2. 中石油工程技术研发有限公司，北京 102206)

(3. 北京浩运金能新能源材料科技有限公司，北京 102100)

**摘　要：**锆具有良好的吸氢性能，被认为是储氘领域的候选材料。但由于其吸氢温度较高且吸氢动力学较慢，目前尚不能进行广泛应用。采用电镀钯的方法对锆进行表面改性，以提高其吸氢性能。结果表明：在经过镀钯且退火处理后的锆合金，在室温下可以实现吸氢，并且有适当的孕育期；与此同时，随着温度的升高，镀钯且退火处理后的锆合金孕育期缩短，吸氢速率变快。通过对微观结构进行分析，发现在氢化后，钯层与锆基板之间形成了过渡区，过渡区中存在$PdH_{1.33}$和$H_{0.62}Zr_{0.38}$。由此可见，过渡区中的氢化物对改善锆的吸氢性能起着重要作用。通过对动力学机制进行研究，确定在室温下，镀钯且退火处理后的锆合金吸氢过程符合一维扩散机制；而在250 ℃时，符合二维扩散机制。

**关键词：**锆；电镀钯；氢吸收温度；氢吸收动力学

作者简介：赵立功，男，1996年生，硕士，北京科技大学新金属材料国家重点实验室，北京 100083，E-mail：1621486848@qq.com